SUPPLEMENTARY DATA

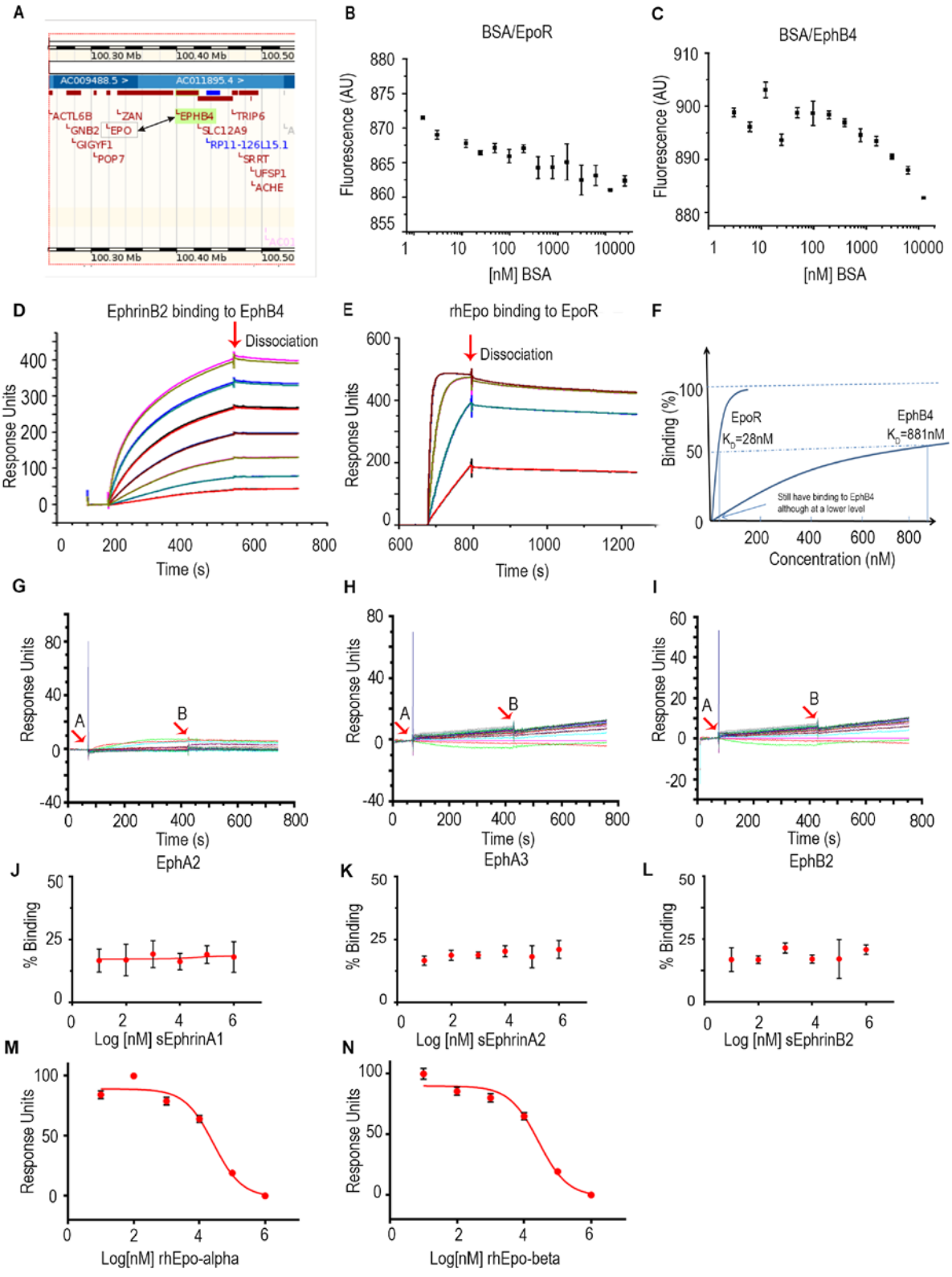

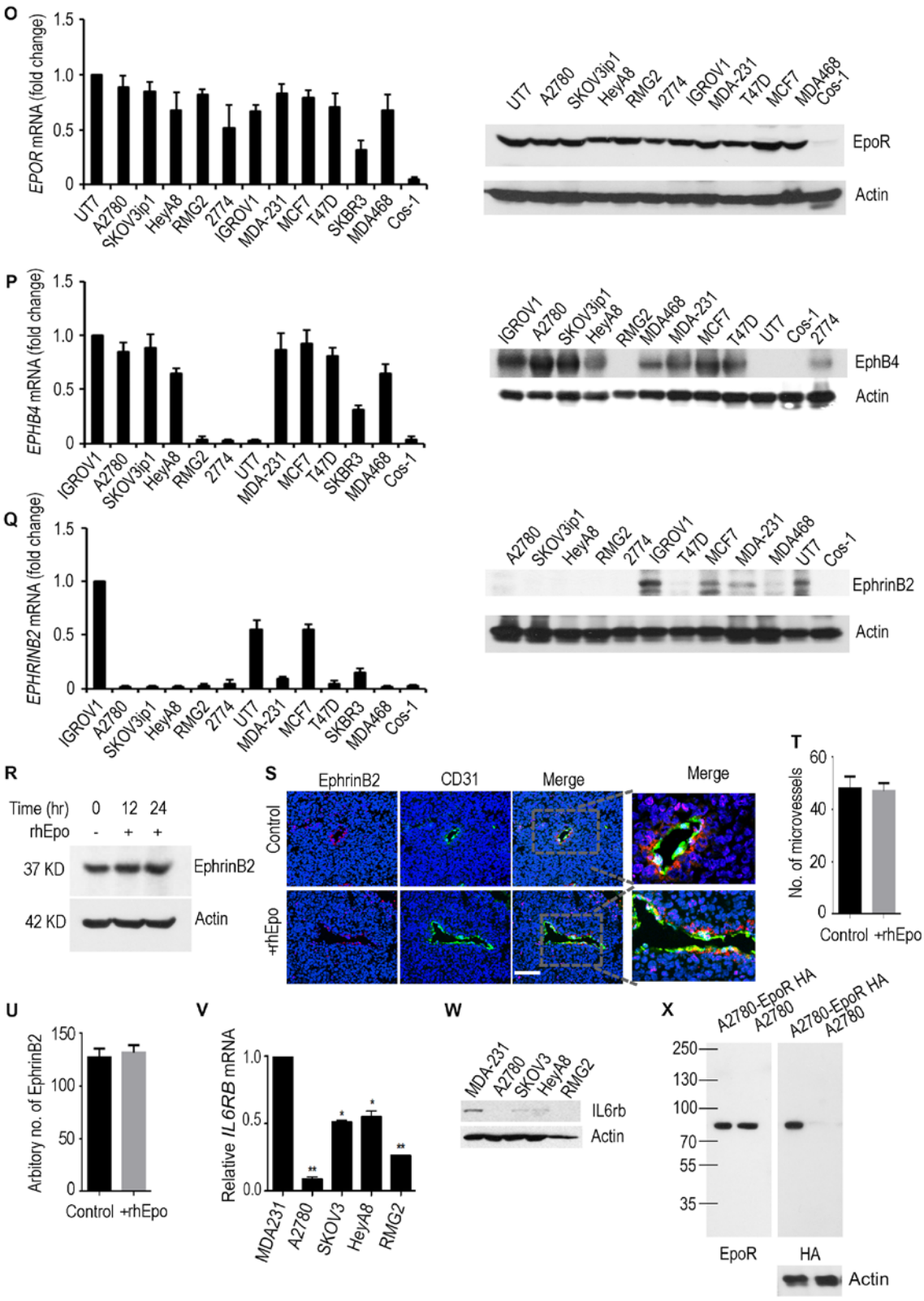
O
EPOR mRNA (fold change)
1.5
1.0
0.5
0
UT7
A2780
SKOV3ip1
HeyA8
RMG2
2774
IGROV1
MDA-231
MCF7
T47D
SKBR3
MDA468
Cos-1
UT7
A2780
SKOV3ip1
HeyA8
RMG2
2774
IGROV1
MDA-231
T47D
MCF7
MDA468
Cos-1
EpoR
Actin
P
EPHB4 mRNA (fold change)
1.5
1.0
0.5
0
IGROV1
A2780
SKOV3ip1
HeyA8
RMG2
2774
UT7
MDA-231
MCF7
T47D
SKBR3
MDA468
Cos-1
IGROV1
A2780
SKOV3ip1
HeyA8
RMG2
MDA468
MDA-231
MCF7
T47D
UT7
Cos-1
2774
EphB4
Actin
Q
EPHRINB2 mRNA (fold change)
1.5
1.0
0.5
0
IGROV1
A2780
SKOV3ip1
HeyA8
RMG2
2774
UT7
MDA-231
MCF7
T47D
SKBR3
MDA468
Cos-1
A2780
SKOV3ip1
HeyA8
RMG2
2774
IGROV1
T47D
MCF7
MDA-231
MDA468
UT7
Cos-1
EphrinB2
Actin
R
Time (hr) 0 12 24
rhEpo - + +
37 KD
42 KD
EphrinB2
Actin
S
EphrinB2
CD31
Merge
Merge
Control
+rhEpo
T
No. of microvessels
60
40
20
0
Control
+rhEpo
U
Arbitory no. of EphrinB2
150
100
50
0
Control
+rhEpo
V
Relative IL6RB mRNA
1.0
0.5
0.0
MDA231
A2780
SKOV3
HeyA8
RMG2
W
MDA-231
A2780
SKOV3
HeyA8
RMG2
IL6rb
Actin
X
A2780-EpoR HA
A2780
A2780-EpoR HA
A2780
250
130
100
70
55
35
EpoR
HA
Actin

Figure S1, related to Figure 1. Evaluation of Epo or EphrinB2 binding to EphB4

(A) Genomic co-localization of the *EPHB4* and *EPO* loci. (B and C) Fluorescence microscale thermophoresis (MST) analysis of BSA controls. (D) Surface Plasmon Resonance (SPR) evaluation of rhEpo or EphrinB2 binding to EphB4. Association and dissociation kinetics of EphrinB2 using the BIAcore instrument. Serial dilutions of peptide from 0.6 nM and 40 nM were injected onto an EphB4-immobilized carboxymethyl dextran biosensor chip. Bound protein is shown as response units (RU) as a function of time. Samples and a buffer blank were injected in duplicate. (E) Binding between Epo and EpoR. Raw sensorgram data for Epo binding to EpoR-Fc on BIAcore. Shown is an overlay of 8 sensorgrams (four concentrations of Epo in range of 13.4 nM to 107 nM in duplicate). EpoR-Fc was captured to sensor chip by mouse anti-human IgG (Fc) antibody. Epo was injected to both control flow cell and EpoR-coated cell, followed by washing with running buffer for 5 min. (F) A hypothetical schematic illustrating the relationship between binding level and ligand concentration. A ligand with low binding affinity may still be able to bind to its corresponding receptor and exert biological functions. Binding Sensorgram of concentration series of rhEpo (0.007-4 μg/mL) to EphA2 (G) EphA3 (H) EphB2 (I) on CM-5 chip. Arrow A represents starting point of sample injection or the beginning of association phase. Arrow B represents the end of sample injection or the beginning of dissociation phase. Competitive binding assays evaluating the binding of EphA2 to EphrinA1 (J), EphA3 to EphrinA2 (K), and EphB2 to EphrinB2 (L) in the presence of rhEpo. Competitive binding assays evaluating rhEpo-alpha (M) and rhEpo-beta (N) binding to EphB4. Western blot and qRT-PCR analysis of (O) EpoR (P) EphB4, and (Q) EphrinB2 expression in ovarian and breast

cancer cell lines and UT7 cells. (R) Western blot analysis of EphrinB2 in endothelial cells. (S) Immunofluorescence staining of EphrinB2 and CD31 in tumors with or without rhEpo (50 IU). Quantification of microvessels (T) and EphrinB2 expression (U) in tumors. (V) qRT-PCR analysis and (W) Western blot analyses of IL6rb in ovarian and breast cancer cell lines. (X) Western blot analysis of ectopically expressed HA tagged EpoR in A2780 cells using HA antibody. Scale bar represents 50 μm. Mean ± SEM values are shown. *$p < 0.05$; **$p < 0.01$. n=3.

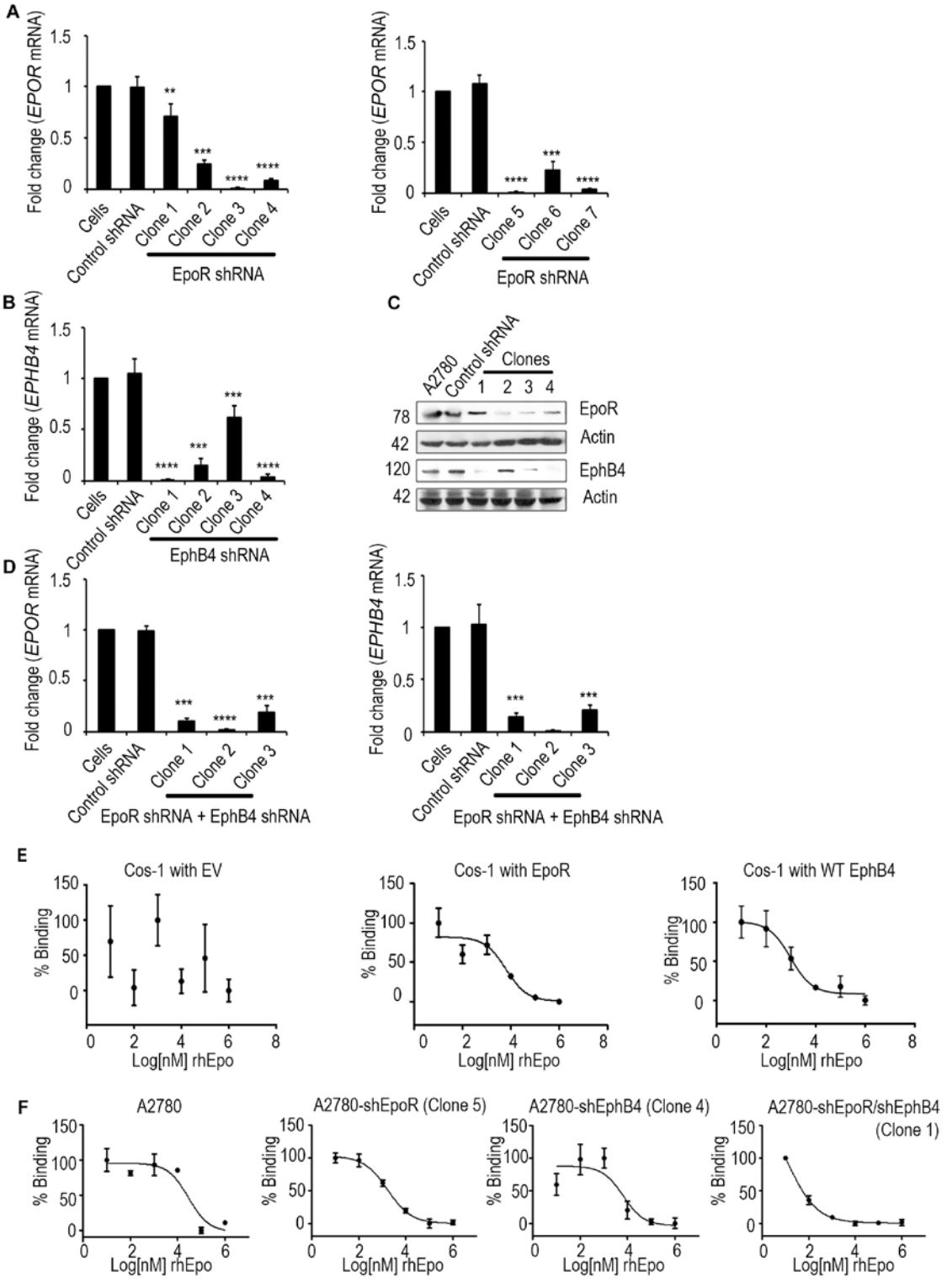
A
Fold change (EPOR mRNA)
Cells
Control shRNA
Clone 1
Clone 2
Clone 3
Clone 4
EpoR shRNA
Clone 5
Clone 6
Clone 7
B
Fold change (EPHB4 mRNA)
EphB4 shRNA
C
A2780
Control shRNA
Clones
1 2 3 4
78
EpoR
42
Actin
120
EphB4
42
Actin
D
EpoR shRNA + EphB4 shRNA
E
Cos-1 with EV
Cos-1 with EpoR
Cos-1 with WT EphB4
% Binding
Log[nM] rhEpo
F
A2780
A2780-shEpoR (Clone 5)
A2780-shEphB4 (Clone 4)
A2780-shEpoR/shEphB4 (Clone 1)

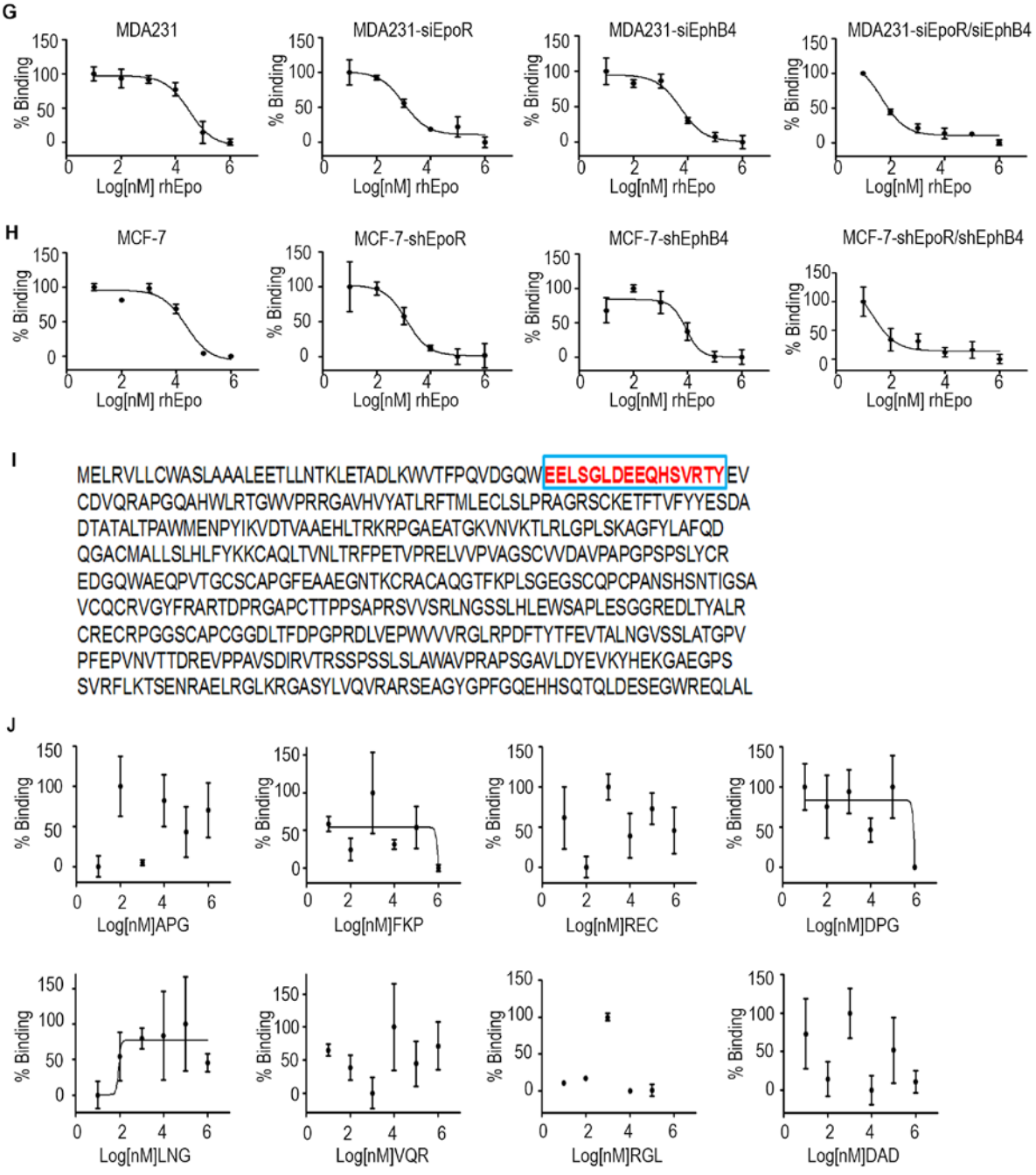
G
MDA231
MDA231-siEpoR
MDA231-siEphB4
MDA231-siEpoR/siEphB4
H
MCF-7
MCF-7-shEpoR
MCF-7-shEphB4
MCF-7-shEpoR/shEphB4
% Binding
Log[nM] rhEpo
I
MELRVLLCWASLAAALEETLLNTKLETADLKWVTFPQVDGQWEELSGLDEEQHSVRTYEV
CDVQRAPGQAHWLRTGWVPRRGAVHVYATLRFTMLECLSLPRAGRSCKETFTVFYYESDA
DTATALTPAWMENPYIKVDTVAAEHLTRKRPGAEATGKVNVKTLRLGPLSKAGFYLAFQD
QGACMALLSLHLFYKKCAQLTVNLTRFPETVPRELVVPVAGSCVVDAVPAPGPSPSLYCR
EDGQWAEQPVTGCSCAPGFEAAEGNTKCRACAQGTFKPLSGEGSCQPCPANSHSNTIGSA
VCQCRVGYFRARTDPRGAPCTTPPSAPRSVVSRLNGSSLHLEWSAPLESGGREDLTYALR
CRECRPGGSCAPCGGDLTFDPGPRDLVEPWVVVRGLRPDFTYTFEVTALNGVSSLATGPV
PFEPVNVTTDREVPPAVSDIRVTRSSPSSLSLAWAVPRAPSGAVLDYEVKYHEKGAEGPS
SVRFLKTSENRAELRGLKRGASYLVQVRARSEAGYGPFGQEHHSQTQLDESEGWREQLAL
J
Log[nM]APG
Log[nM]FKP
Log[nM]REC
Log[nM]DPG
Log[nM]LNG
Log[nM]VQR
Log[nM]RGL
Log[nM]DAD

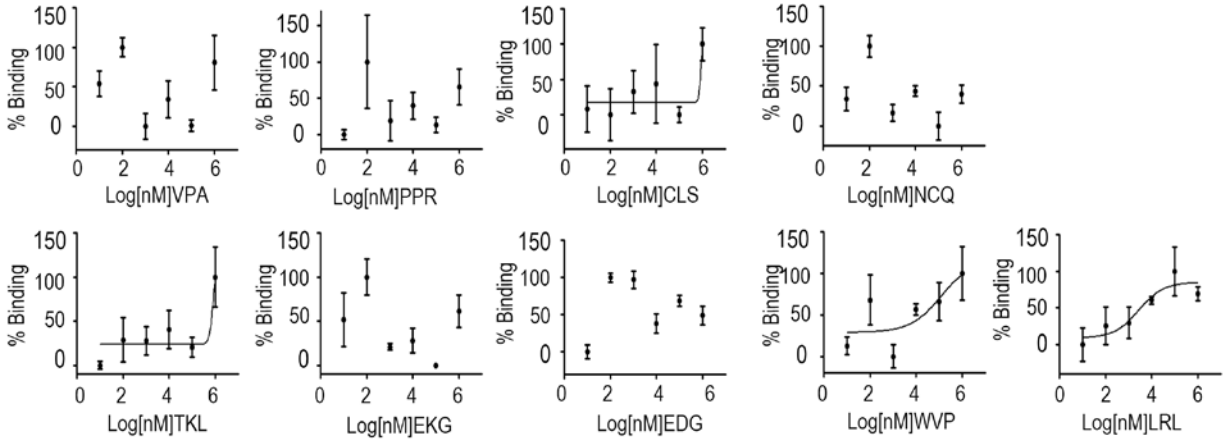
% Binding
Log[nM]VPA
Log[nM]PPR
Log[nM]CLS
Log[nM]NCQ
Log[nM]TKL
Log[nM]EKG
Log[nM]EDG
Log[nM]WVP
Log[nM]LRL

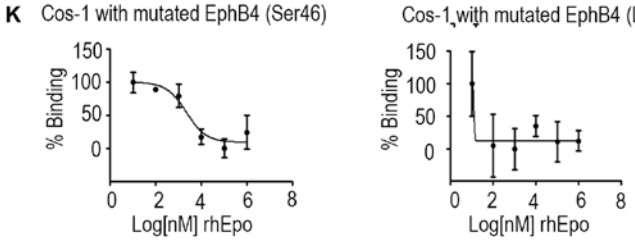
K
Cos-1 with mutated EphB4 (Ser46)
Cos-1 with mutated EphB4 (Leu48)
% Binding
Log[nM] rhEpo

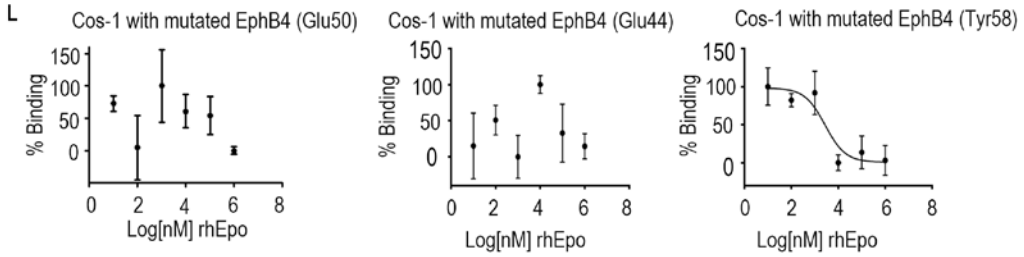
L
Cos-1 with mutated EphB4 (Glu50)
Cos-1 with mutated EphB4 (Glu44)
Cos-1 with mutated EphB4 (Tyr58)
% Binding
Log[nM] rhEpo

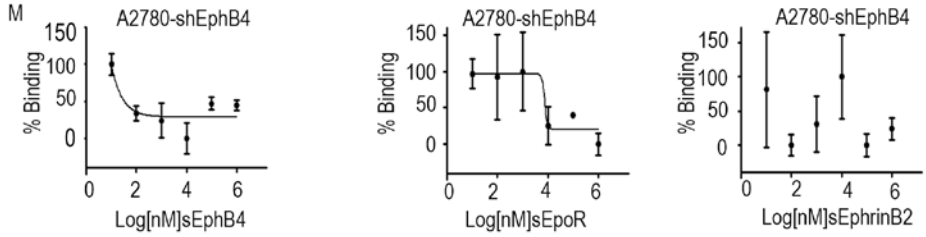
M
A2780-shEphB4
% Binding
Log[nM]sEphB4
Log[nM]sEpoR
Log[nM]sEphrinB2

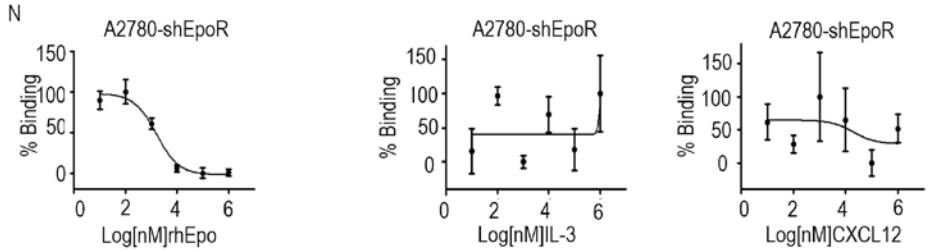
N
A2780-shEpoR
% Binding
Log[nM]rhEpo
Log[nM]IL-3
Log[nM]CXCL12

Figure S2, related to Figure 2. Characterization of rhEpo binding to ovarian and breast cancer cells

(A) Real-time RT-PCR analysis of *EPOR* expression in A2780-shEpoR cells. (B) Real-time RT-PCR analysis of *EphB4* expression in A2780-shEphB4 cells. (C) Western blot analyses of EpoR and EphB4 expression in A2780-shEpoR and -shEphB4 cells (numbers on the left represent molecular weights). (D) Real-time RT-PCR analysis of *EPOR* and *EPHB4* expression in A2780 cells transfected with shEpoR and shEphB4. (E) Binding of [I^{125}]rhEpo to Cos-1 cells transfected with empty vector, EpoR, or EphB4. (F) Binding of [I^{125}]rhEpo to A2780-shEpoR (clone 5), A2780-shEphB4 (clone 4), and A2780-shEpoR/shEphB4 (clone 2). (G) Binding of [I^{125}]rhEpo to MDA-MB231, MDA-MB231-siEpoR, MDA-MB231-siEphB4, and MDA-MB231-siEpoR/siEphB4. (H) Binding of [I^{125}]rhEpo to MCF-7, MCF-7-shEpoR, MCF-7-shEphB4, and MCF-7-shEpoR/shEphB4. (I) Localization of the competitive peptides within the extracellular domain of EphB4. (J) Competitive binding assays between [I^{125}]rhEpo and different peptides in A2780-shEpoR cells. (K) Binding of [I^{125}]rhEpo to Cos-1 cells transfected with mutant EphB4 (Ser46, or Leu 48) at EphrinB2-EphB4 binding domain. (L) Binding of [I^{125}]rhEpo to Cos-1 cells transfected with mutant EphB4 (Glu50, Glu44 or Tyr58) at EphrinB2-EphB4 binding domain. (M) Competitive binding between [I^{125}]rhEpo and soluble EphrinB2, soluble EpoR, or soluble EphrinB2 in A2780-shEphB4 cells. (N) Competitive binding between [I^{125}]rhEpo and rhEpo, IL3, or CXCL12. Mean ± SEM values are shown. **$p < 0.01$, ***$p < 0.001$, ****$p < 0.0001$. n=3.

Table S1, related to Figure 2. EphB4 mutation in EEL domain

EphB4 mutation on EEL domain	
EEL	GAG GAA CTG AGC GGC CTG GAT GAG GAA CAG CAC AGC GTG CGC ACC TAC E E L S G L D E E Q H S V R T Y
Glu-44→-Ser-44	GAG TCG CTG AGC GGC CTG GAT GAG GAA CAG CAC AGC GTG CGC ACC TAC E S L S G L D E E Q H S V R T Y
Ser-46→Ala-46	GAG GAA CTG GCC GGC CTG GAT GAG GAA CAG CAC AGC GTG CGC ACC TAC E E L A G L D E E Q H S V R T Y
Leu-48→Tyr-48	GAG GAA CTG AGC GGC TAC GAT GAG GAA CAG CAC AGC GTG CGC ACC TAC E E L S G Y D E E Q H S V R T Y
Glu-50→Ser-50	GAG GAA CTG AGC GGC TAC GAT TCG GAA CAG CAC AGC GTG CGC ACC TAC E E L S G L D S E Q H S V R T Y
Tyr-58->Leu-58	GAG GAA CTG AGC GGC CTG GAT GAG GAA CAG CAC AGC GTG CGC ACC CTG E E L S G L D E E Q H S V R T L

Table S2, related to Figure 2. Raw data of binding assay

Provided as a separate Excel file

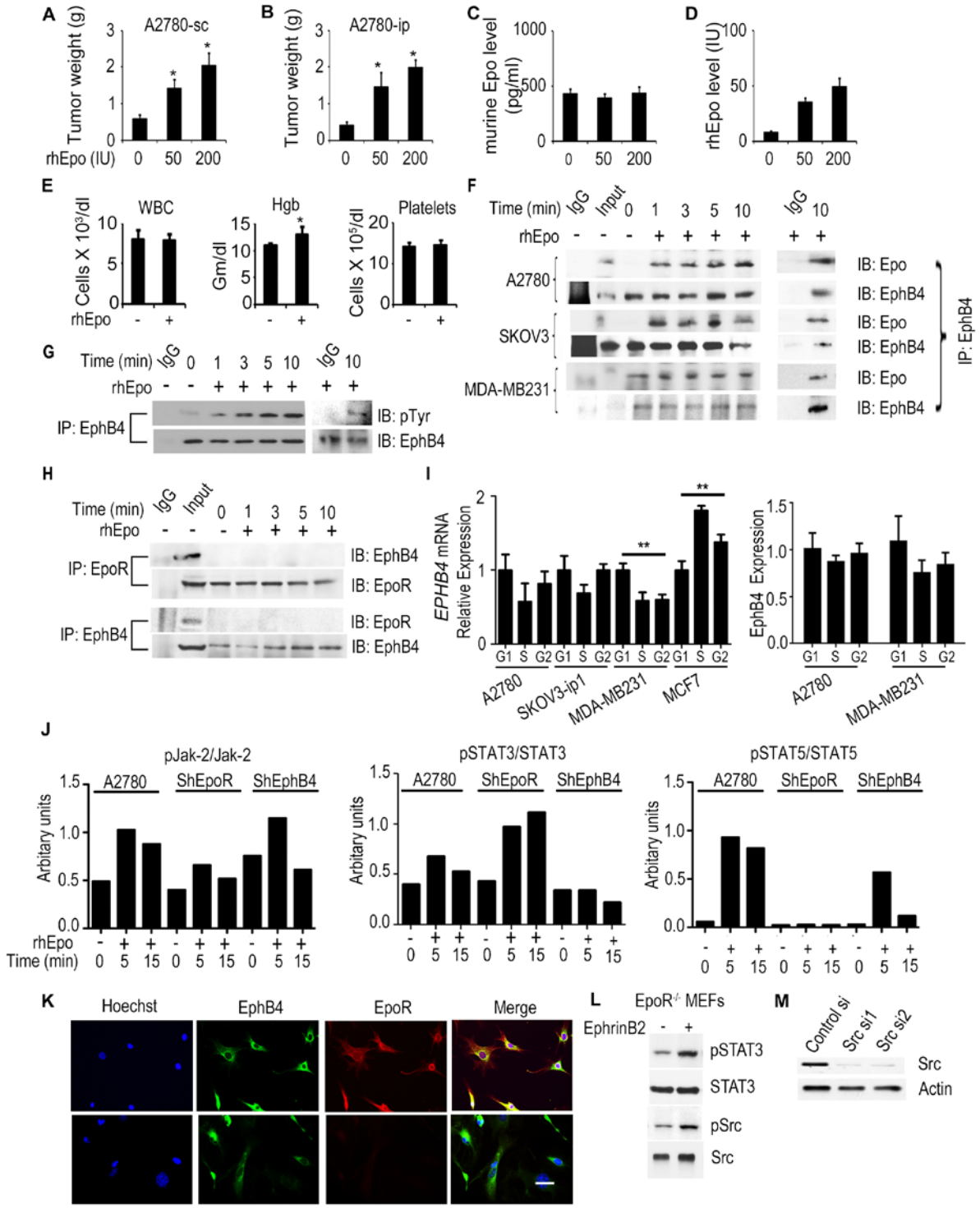
A
A2780-sc
Tumor weight (g)
rhEpo (IU) 0 50 200
B
A2780-ip
Tumor weight (g)
C
murine Epo level (pg/ml)
D
rhEpo level (IU)
E
WBC
Cells X 10³/dl
Hgb
Gm/dl
Platelets
Cells X 10⁵/dl
rhEpo
F
Time (min) IgG Input 0 1 3 5 10 IgG 10
rhEpo
A2780
SKOV3
MDA-MB231
IB: Epo
IB: EphB4
IP: EphB4
G
Time (min) IgG 0 1 3 5 10 IgG 10
rhEpo
IP: EphB4
IB: pTyr
IB: EphB4
H
Time (min) IgG Input 0 1 3 5 10
rhEpo
IP: EpoR
IP: EphB4
IB: EphB4
IB: EpoR
I
EPHB4 mRNA Relative Expression
G1 S G2
A2780
SKOV3-ip1
MDA-MB231
MCF7
EphB4 Expression
J
pJak-2/Jak-2
pSTAT3/STAT3
pSTAT5/STAT5
A2780 ShEpoR ShEphB4
Arbitary units
rhEpo
Time (min)
K
Hoechst
EphB4
EpoR
Merge
L
EpoR-/- MEFs
EphrinB2
pSTAT3
STAT3
pSrc
Src
M
Control si
Src si1
Src si2
Src
Actin

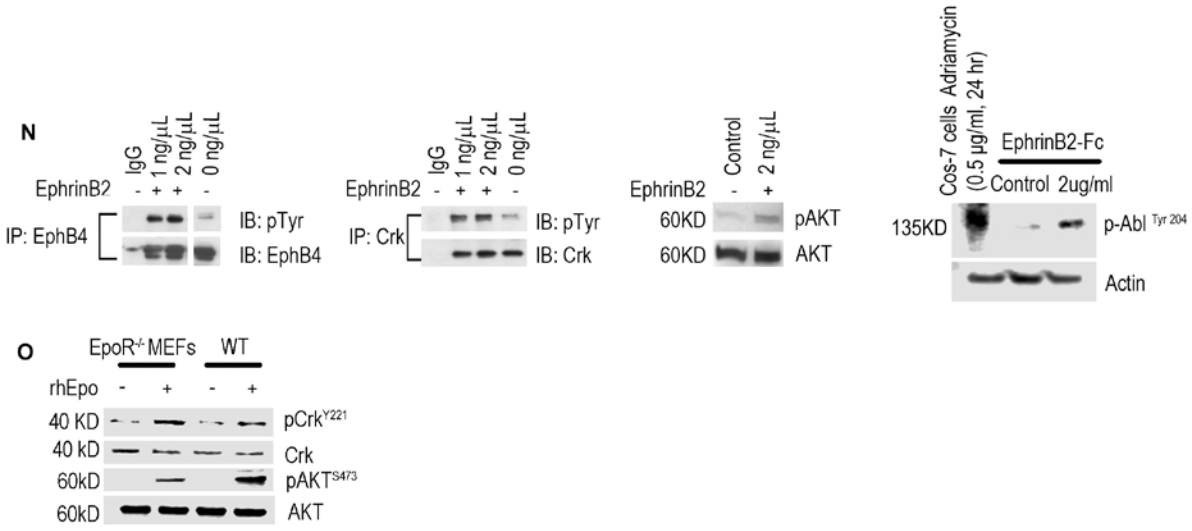

Figure S3, related to Figure 3. Characterization of rhEpo-mediated activation of EphB4

Effect of rhEpo dose on the growth of A2780 tumors injected into the subcutaneous space (A, A2780-sc) or into the peritoneal cavity of nude mice (B, A2780-ip); n=10, (C) murine Epo levels and (D) human Epo levels in tumors. (E) Evaluation of white blood cells (WBC), hemoglobin (Hgb), and platelets in mice bearing A2780 tumors treated with intraperitoneal (i.p.) rhEpo. The rhEpo treatment was given 3x/week for 3 weeks. (F) Interaction between rhEpo and EphB4 in ovarian (A2780 and SKOV3) and breast (MDA-MB231) cancer cell lines. (G) Activation of EphB4 by rhEpo in MDA-MB231 cells. (H) A2780 parental cells were stimulated with rhEpo (50 IU/mL) for indicated time points. Interaction between EpoR and EphB4 were analyzed by immunoprecipitation assay. (I) mRNA assessment of *EPHB4* expression in cancer cells (A2780, SKOV3-ip1, MDA-MB231, and MCF7) at different stages of cell cycle. A2780 and MDA-MB231 cells were labeled with EphB4 antibody and FACS sorted according to cell cycle. Dose of rhEpo used for both experiments was 50 IU/mL. (J) Densitometry image analysis of

pJak2, pSTAT5, and pSTAT3 levels in A2780, A2780-shEpoR, and -shEphB4 cells following rhEpo treatment (also see Figure 3b). (K) Immunofluorescence staining using EphB4 (green) and EpoR (red) antibody in $EpoR^{-/-}$ MEFs. Scale bar represents 50 µm. (L) Western blot analysis for STAT3 following rhEpo stimulation in $EpoR^{-/-}$ MEFs. (M) Western blot analysis for Src following siSrc transfection in A2780 cells. (N) Effect of EphrinB2 on EphB4, Crk, Akt, and Abl activation along with positive control. (O) Effect of rhEpo on Crk and Akt activation in $EpoR^{-/-}$MEFs. Mean ± SEM values are shown. *$p < 0.05$; **$p < 0.01$.

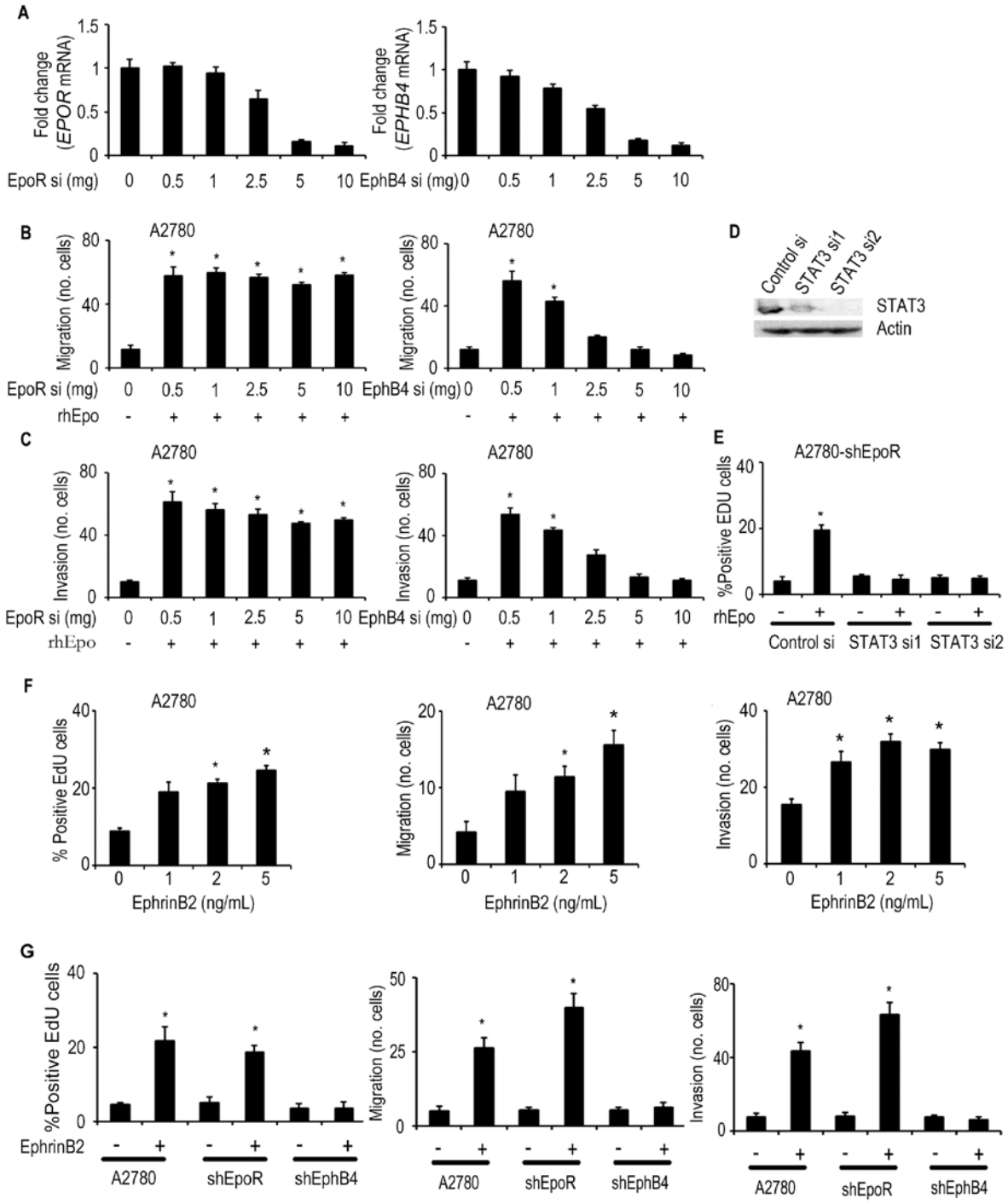
A
Fold change (EPOR mRNA)
EpoR si (mg) 0 0.5 1 2.5 5 10
Fold change (EPHB4 mRNA)
EphB4 si (mg) 0 0.5 1 2.5 5 10
B
A2780
Migration (no. cells)
EpoR si (mg) 0 0.5 1 2.5 5 10
rhEpo - + + + + +
EphB4 si (mg) 0 0.5 1 2.5 5 10
D
Control si
STAT3 si1
STAT3 si2
STAT3
Actin
C
Invasion (no. cells)
E
A2780-shEpoR
%Positive EDU cells
Control si
STAT3 si1
STAT3 si2
F
% Positive EdU cells
EphrinB2 (ng/mL)
G
%Positive EdU cells
EphrinB2
A2780
shEpoR
shEphB4

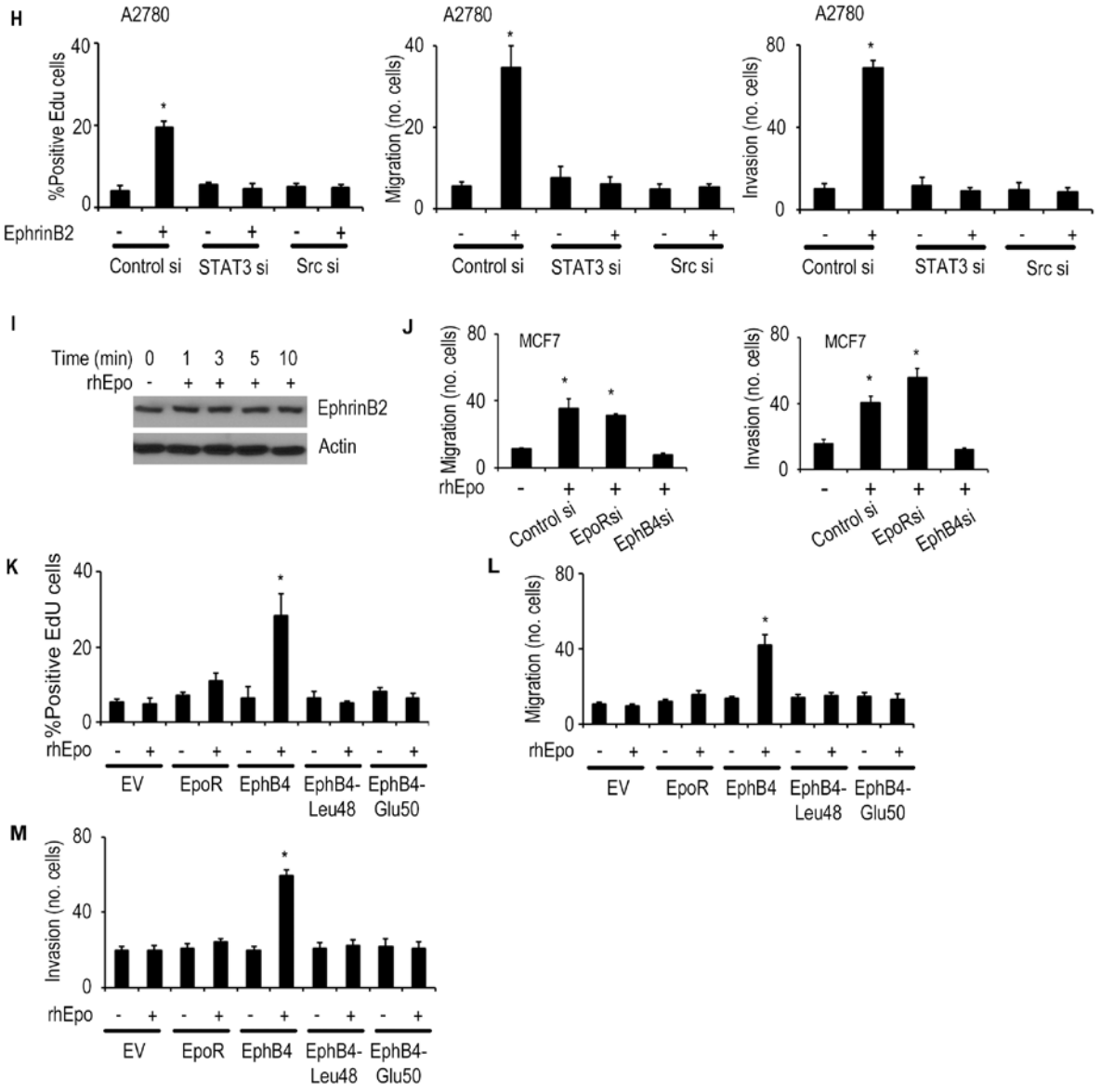

Figure S4, related to Figure 4. rhEpo-mediated effects on cancer cells

(A) Dose-dependent effects of *EPOR* or *EPHB4* siRNA on mRNA levels of respective genes in A2780 cells. (B-C) Dose-dependent effects of EpoR or EphB4 siRNA on migration and invasion of A2780 cells in the presence or absence of rhEpo. (D) Western blot analysis of STAT3 following siSTAT3 transfection in A2780 cells. (E) Effect of STAT3 siRNA on proliferation of A2780 cells in the presence or absence of rhEpo. The

dose of rhEpo used for these experiments was 50 IU/mL. (F) Effect of EphrinB2 on proliferation, migration, and invasion of A2780 cells. (G) Proliferation, migration, and invasion of A2780 parental, -shEpoR, and -shEphB4 cells in the presence or absence of EphrinB2. (H) Effect of STAT3 or Src siRNA on proliferation, migration, and invasion of A2780 parental cells in the presence or absence of EphrinB2. (I) Effect of rhEpo on EphrinB2 expression levels in MDA-MB231 cells. (J) Effect of EpoR or EphB4 silencing on migration and invasion of MCF7 cells. (K) Proliferation, (L) migration, and (M) invasion of Cos-1 cells transfected with EphB4, EpoR or EphB4 mutant (Leu48 or Glu50). Mean ± SEM values are shown. Mann-Whitney rank sum test *$p < 0.001$.

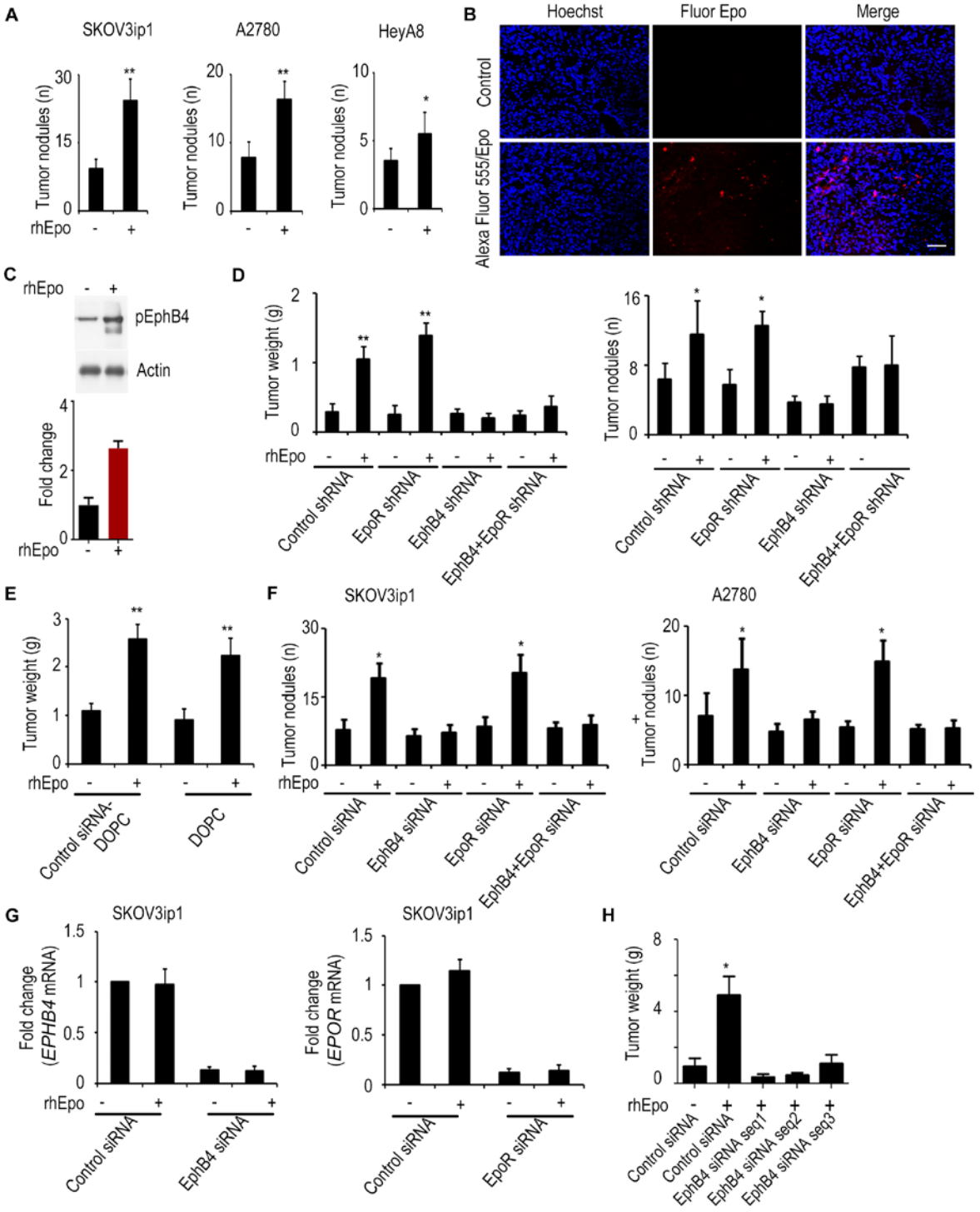
A
SKOV3ip1
A2780
HeyA8
Tumor nodules (n)
rhEpo
B
Hoechst
Fluor Epo
Merge
Control
Alexa Fluor 555/Epo
C
rhEpo
pEphB4
Actin
Fold change
D
Tumor weight (g)
Tumor nodules (n)
Control shRNA
EpoR shRNA
EphB4 shRNA
EphB4+EpoR shRNA
E
Control siRNA-DOPC
DOPC
F
SKOV3ip1
A2780
Control siRNA
EphB4 siRNA
EpoR siRNA
EphB4+EpoR siRNA
G
SKOV3ip1
Fold change (EPHB4 mRNA)
Fold change (EPOR mRNA)
H
Tumor weight (g)
Control siRNA
EphB4 siRNA seq1
EphB4 siRNA seq2
EphB4 siRNA seq3

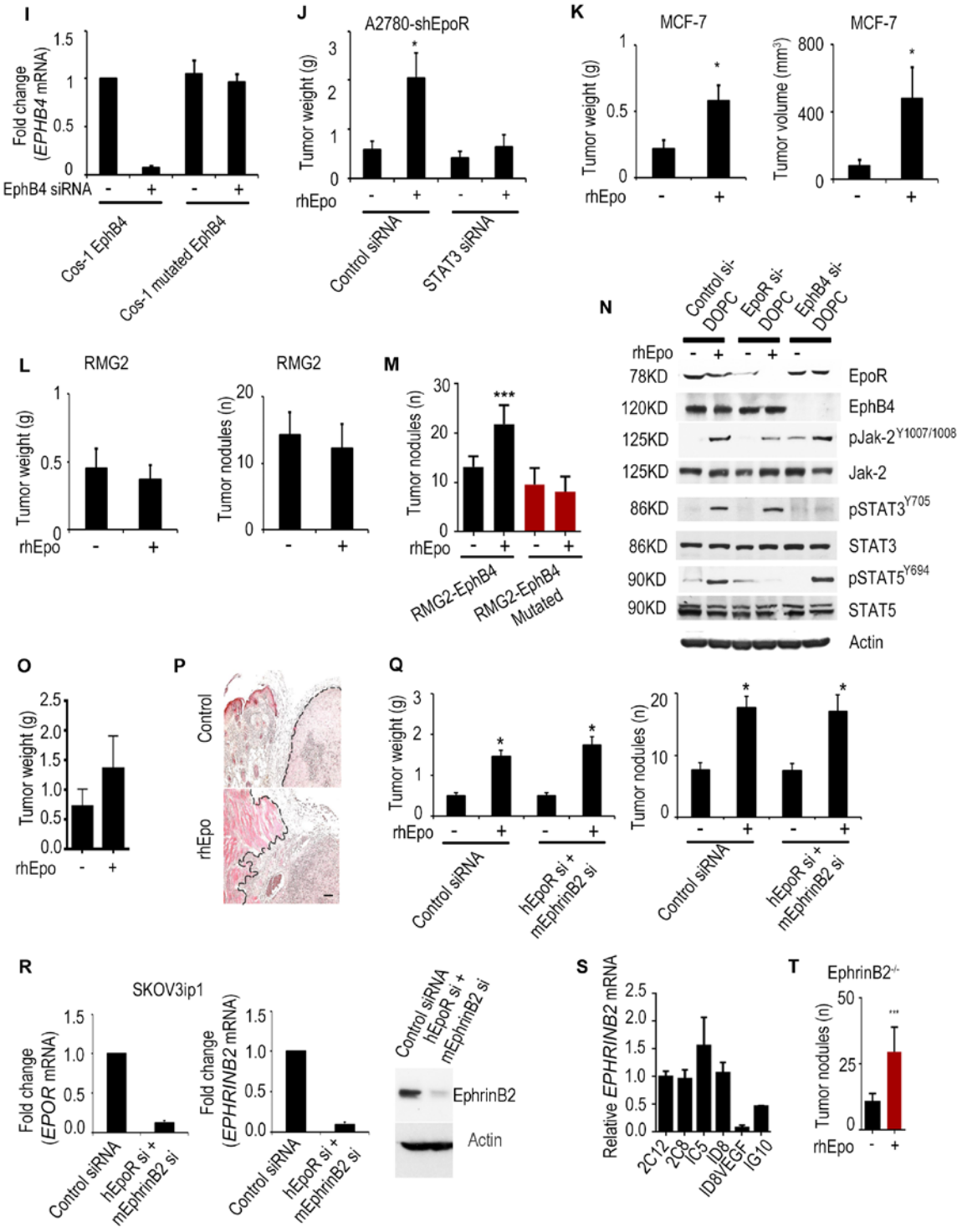
I
Fold change (EPHB4 mRNA)
EphB4 siRNA
Cos-1 EphB4
Cos-1 mutated EphB4
J
A2780-shEpoR
Tumor weight (g)
rhEpo
Control siRNA
STAT3 siRNA
K
MCF-7
Tumor weight (g)
MCF-7
Tumor volume (mm3)
L
RMG2
Tumor weight (g)
RMG2
Tumor nodules (n)
M
Tumor nodules (n)
RMG2-EphB4
RMG2-EphB4 Mutated
N
Control si-DOPC
EpoR si-DOPC
EphB4 si-DOPC
78KD EpoR
120KD EphB4
125KD pJak-2Y1007/1008
125KD Jak-2
86KD pSTAT3Y705
86KD STAT3
90KD pSTAT5Y694
90KD STAT5
Actin
O
Tumor weight (g)
P
Control
rhEpo
Q
Tumor weight (g)
Tumor nodules (n)
Control siRNA
hEpoR si + mEphrinB2 si
R
SKOV3ip1
Fold change (EPOR mRNA)
Fold change (EPHRINB2 mRNA)
EphrinB2
Actin
S
Relative EPHRINB2 mRNA
2C12
2C8
IC5
ID8
ID8VEGF
IG10
T
EphrinB2-/-
Tumor nodules (n)

Figure S5, related to Figure 5. *In vivo* EphB4 silencing blocks rhEpo-induced tumor growth

(A) Effect of rhEpo on number of nodules in SKOV3ip1, A2780, and HeyA8 orthotopic mouse models. (B) Histological analysis of tumor following fluorescently labelled (Alexa Flour 555) rhEpo treatment. (C) Western blot of pEphB4 in tumors after rhEpo administration in mice bearing A2780 tumors. Adjacent graph shows the quantification pEphB4. (D) Seven days following injection of A2780-shControl, -shEphB4, -shEpoR, or -dual shEpoR + shEphB4 cells into the peritoneal cavity (n = 10 mice per group), mice were treated with either vehicle control or rhEpo (50 IU given 3x/week i.p.). A necropsy was performed after 5 weeks and aggregate tumor weight and number of nodules were assessed. (E) Effect of empty DOPC nanoliposomes or control siRNA-DOPC (150 µg/kg i.p. given twice weekly for 5 weeks) on A2780 tumor growth *in vivo* with or without rhEpo (50 IU given 3x/week i.p.). (F) Effect of control, EphB4, EpoR or EphB4 + EpoR siRNAs on tumor growth in the presence or absence of rhEpo in SKOV3ip1 or A2780 mice models. (G) Effect of EphB4 and EpoR siRNAs on *EPHB4* and *EPOR* mRNA levels, respectively, in the SKOV3ip1 model *in vivo*. (H) Evaluation of the effect of different siRNA sequences of EphB4 on the inhibition of rhEpo-induced tumor growth *in vivo.* A2780 tumor-bearing (peritoneal cavity) animals (n = 10 mice per group) were treated with either control siRNA or different EphB4 targeted siRNA sequences (150 µg/kg i.p. given twice weekly for 5 weeks) in DOPC nanoliposomes. The rhEpo was given at 50 IU given 3x/week i.p. A necropsy was performed to assess aggregate tumor weight at the end of the experiment. (I) *EPHB4* expression (qRT-PCR) following EphB4 siRNA treatment in Cos-1 cells transfected with either an EphB4 or mutated EphB4

construct. (J) Effect of control or STAT3 siRNAs on tumor growth in the presence or absence of rhEpo in A2780-shEpoR model. (K) Effect of rhEpo (50 IU given 3x/week i.p.) on tumor growth in the MCF-7 breast cancer mouse model. (L) Effect of rhEpo on RMG2 ovarian cancer model. (M) Number of tumor nodules following intraperitoneal injection of ectopically expressed EphB4 or the mutated form of EphB4 in RMG2 model. (N) Expression of EpoR or EphB4 downstream targets in tumors obtained from mice bearing A2780 tumors treated with control siRNA-DOPC, EpoR siRNA-DOPC, or EphB4 siRNA-DOPC with or without rhEpo (50 IU given 3x/week i.p.; n=10 mice per group). Tumor samples from each group were subjected to Western blot analyses for the proteins listed on the figure. (O) Tumor weight following rhEpo treatment. (P) H and E staining shows invasion of tumor cells into muscle layer. (Q) Mice bearing SKOV3ip1 (EphrinB2-negative) tumors were treated with either control or hEpoR + mEphrinB2 siRNAs incorporated in chitosan nanoparticles (150 µg/kg i.p. twice weekly). rhEpo was given at 50 IU given 3x/week i.p. (R) Effect of hEpoR and mEphrinB2 siRNAs on *EPOR* and *EPHRINB2* expression levels are shown. (S) Relative mRNA expression of *EPHRINB2* in murine cell lines. (T) Effect of rhEpo on number of ID8VEGF tumor nodules in EphrinB2$^{-/-}$ mice. Scale bar represents 50 µm. n=10, Mean ± SEM values are shown. *p<0.05; **p<0.001, ***p <0.001.

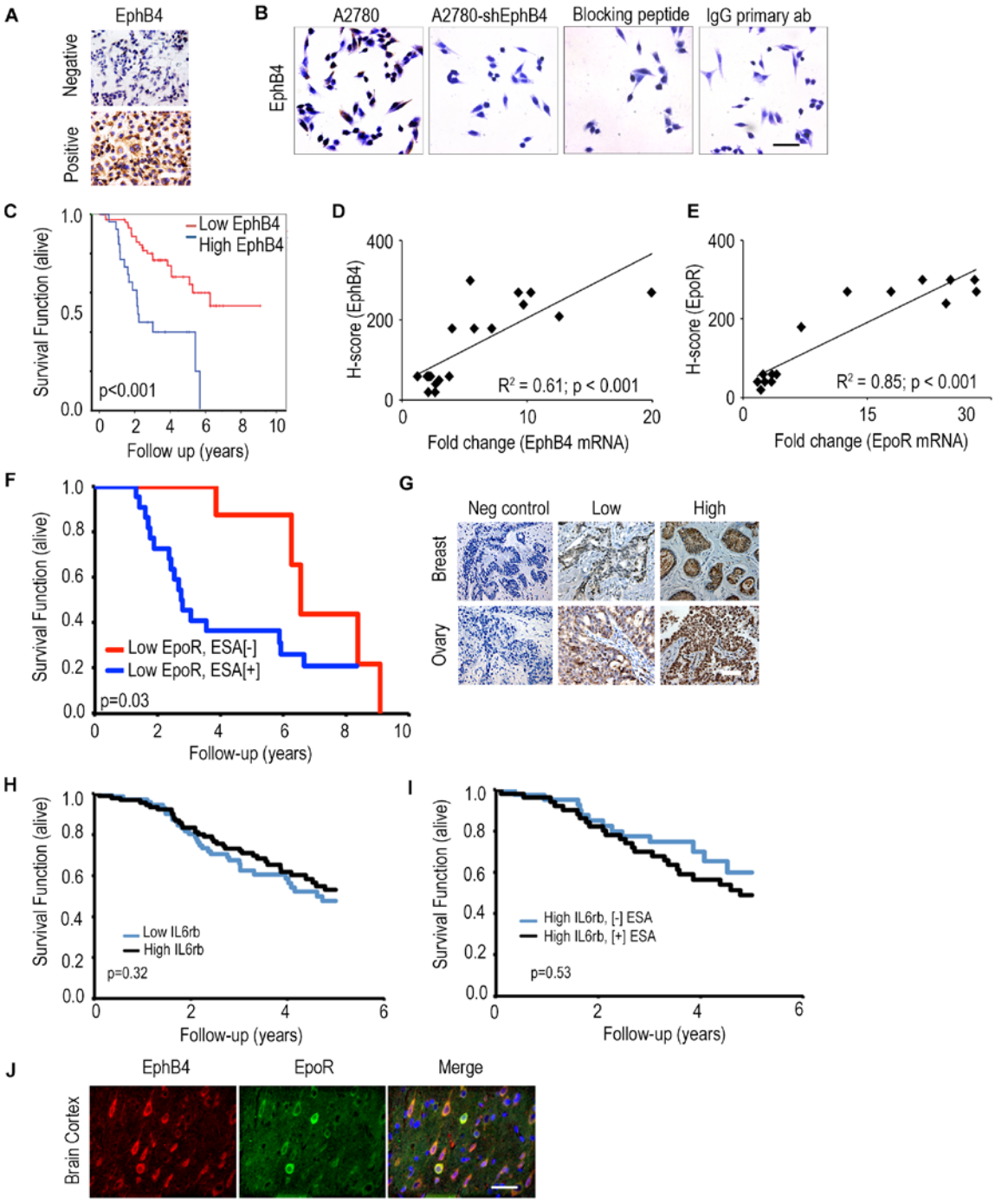
A
EphB4
Negative
Positive
B
A2780
A2780-shEphB4
Blocking peptide
IgG primary ab
EphB4
C
Survival Function (alive)
Low EphB4
High EphB4
p<0.001
Follow up (years)
D
H-score (EphB4)
R² = 0.61; p < 0.001
Fold change (EphB4 mRNA)
E
H-score (EpoR)
R² = 0.85; p < 0.001
Fold change (EpoR mRNA)
F
Survival Function (alive)
Low EpoR, ESA[-]
Low EpoR, ESA[+]
p=0.03
Follow-up (years)
G
Neg control
Low
High
Breast
Ovary
H
Survival Function (alive)
Low IL6rb
High IL6rb
p=0.32
Follow-up (years)
I
Survival Function (alive)
High IL6rb, [-] ESA
High IL6rb, [+] ESA
p=0.53
Follow-up (years)
J
EphB4
EpoR
Merge
Brain Cortex

Figure S6, related to Figure 6. Correlation of EphB4 and EpoR protein and mRNA expression

(A) Immunohistochemical staining using EphB4 antibody in IGROV cells with or without EphB4 siRNA transfection. Scale bar represents 50 µm (B) Immunohistochemical staining using EphB4 antibody (Thermoscientific MA5-15506) on A2780 or A2780-shEphB4 cells with either blocking peptide or IgG primary antibody. Scale bar represents 200 µm. (C) To confirm the clinical relevance of EphB4 expression, we also carried out staining with an alternate antibody (Thermoscientific MA5-15506) in a subset of the ovarian cancer samples (n=105) presented in Figure 6E. Data from this analysis were then plotted using the Kaplan-Meier method. These results were similar the ones in Figure 6E. (D and E) EphB4 or EpoR protein expression is plotted against *EPHB4* or *EPOR* mRNA expression in human epithelial ovarian cancer samples (n=19). (F) Kaplan-Meier curve of disease-specific survival of ovarian cancer patients with low tumoral expression of EpoR, stratified by treatment with ESA. The log-rank test (two-sided) was used to compare differences between groups. (G) Immunohistochemical peroxidase staining of IL6rb in human ovarian and breast cancer samples. Scale bar represents 50 µm (H) Kaplan-Meier curve of disease-specific mortality for ovarian cancer patients stratified by tumoral IL6rb expression. (I) Kaplan-Meier curve of disease-specific mortality of ovarian cancer patients stratified by IL6rb expression ESA treatment. The log-rank test (two-sided) was used to compare differences between groups. (J) Rat brain cortex stained with EphB4 and EpoR antibodies. Scale bar represents 200 µm.

Table S3, related to Figure 6. Demographic and clinical characteristics of the cohort of patients with epithelial ovarian cancer; data are presented based on EphB4 and EpoR expression level.

	Low Ephb4	**High EphB4**	***p**	**Low EpoR**	**High EpoR**	***p**
Diagnosis						
Ovarian	94 (90.4%)	66 (95.7%)	0.25	32 (88.9%)	128 (93.4%)	0.47
Peritoneal	10 (9.6%)	3 (4.4%)		4 (11.1%)	9 (6.6%)	
Stage						
I	5 (4.7%)	1 (1.5%)	0.41	2 (5.4%)	4 (2.9%)	0.61
II, III, IV	101 (95.3%)	68 (98.6%)		35 (94.6%)	134 (97.1%)	
Grade						
Low	6 (5.7%)	10 (14.5%)	0.06	5 (13.9%)	11 (8%)	0.33
High	99 (94.3%)	59 (85.5%)		31 (86.1%)	127 (92%)	
Histology						
Serous	90 (84.9%)	59 (85.5%)	1.00	31 (83.8%)	118 (85.5%)	0.80
Other	16 (15.1%)	10 (14.5%)		6 (16.2%)	20 (14.5)	
Ascites						
No	43 (40.6%)	28 (44.4%)	0.63	14 (41.2%)	57 (42.2%)	1.00
Yes	63 (59.4%)	35 (55.6%)		20 (58.8%)	78 (57.8%)	
Cytoreduction						
Suboptimal	30 (28.3%)	28 (40.1%)	0.10	13 (35.1%)	45 (32.6%)	0.85
Optimal	76 (71.2%)	41 (59.4%)		24 (64.9%)	93 (67.4%)	
CA125						
Mean (SD)	2103 (5825)	2364 (5058)	0.08	1051 (1461)	2418 (6047)	0.33
Age						
Median (Range)	59 (20-92)	56 (26-88)	0.03*	55 (26-88)	59 (20-92)	0.08
Low EpoR	18 (17%)	19 (27.5%)	0.13			
High EpoR	88 (83%)	50 (72.5%)				
Low EphB4				18 (48.6%)	86 (63.8%)	0.13
High EphB4				19 (51.4%)	50 (36.2%)	

*Comparison made with the Fisher's exact test. All p values are two-sided.

Table S4, related to Figure 6. Summary statistics for disease-specific survival and death in the ovarian cancer cohort.

Provided as a separate Excel file

Table S5, related to Figure 6. Demographic and clinical characteristics of the cohort of patients with breast cancer; data are presented based on EphB4 and EpoR expression level.

	Low EphB4 (n=22)	**High EphB4 (n=66)**	**P**	**Low EpoR (n=19)**	**High EphB4 (n=69)**	**P**
Median Age (Range)	54.8 (23.6-73.2)	54.3 (14.5-73.8)	0.80	54.5 (14.5-73.8)	54 (14.5-73.8)	0.56
Stage						
I	6 (27.3%)	20 (30.3%)	0.71	5 (26.3%)	21 (30.4%)	0.80
II	11 (50%)	27 (40.9%)		9 (47.4%)	29 (42.0%)	
III	3 (13.6%)	15 (22.7%)		3 (15.8%)	15 (21.7%)	
IV	2 (9.1%)	4 (6.1%)		2 (10.5%)	4 (5.8%)	
Low EpoR	5 (22.7%)	14 (21.2%)	1.00			
High EpoR	17 (77.3%)	52 (78.8%)				
Low EphB4				5 (26.3%)	17 (24.6%)	1.00
High EphB4				14 (73.7%)	52 (75.4%)	

Table S6, related to Figure 6. Summary statistics for disease-free survival in the breast cancer cohort.

	Expression	n	# of Events	Median time to event (yrs)	*p
EphB4	Low	22	0		<0.01
	High	66	25	9.4	
EpoR	Low	19	6	7.2	0.74
	High	69	19	10.1	
EphB4 and EpoR	Low EpoR/Low EphB4	5	0		0.03
	Low EpoR/High EphB4	14	6	7.2	
	High EpoR/Low EphB4	17	0		
	High EpoR/High EphB4	52	19	9.4	
Epo treatment (All Patients)	No	56	5		<0.001
	Yes	32	20	6.2	
Epo treatment (High EphB4)	No	39	5		<0.01
	Yes	27	20	5.7	
Epo treatment (High Epo R)	No	45	4		<0.001
	Yes	24	15	6.2	

***Comparison made using log-rank statistic

Table S7, related to Figure 6: Summary statistics for disease-free survival in the breast cancer cohort by receptor status

	Expression	n	# of events	Log-rank test	HR (95%CI)	*p
ER	Negative	13	4	Referent		
	Positive	23	2	0.1286	0.29 (0.05-1.60)	0.1561
EpoR	Low	14	3	Referent		
	High	52	13	0.6911	1.29 (0.37-4.52)	0.6935
ER and EpoR	ER: Negative, EpoR: Low	5	1	Referent		
	ER: Negative, EpoR: High	8	3		NE	NE
	ER: Positive, EpoR: Low	2	0		NE	NE
	ER: Positive, EpoR: High	21	2	0.3266	NE	NE
Her2	Negative	28	4	Referent		
	Positive	10	2	0.5528	1.66 (0.30-9.11)	0.5592
Her2 and EpoR	Her2: Negative, EpoR: Low	5	1	Referent		
	Her2: Negative, EpoR: High	8	3		NE	NE
	Her2: Positive, EpoR: Low	2	0		NE	NE
	Her2: Positive, EpoR: High	21	2	0.3266	NE	NE
ESA treatment	No	39	4	Referent		
	Yes	27	12	0.0079	4.09 (1.32-12.68)	0.0148
ESA treatment (negative ER)	No	10	3	Referent		
	Yes	3	1	0.9515	0.93 (0.10-8.99)	0.9515
ESA treatment (positive ER)	No	17	0	Referent		
	Yes	6	2	0.0588	NE	NE
ESA treatment (negative Her2)	No	22	1	Referent		
	Yes	6	3	0.0115	10.3 (1.07-98.76)	0.0439
ESA treatment (positive Her2)	No	8	2	Referent		
	Yes	2	0	0.4315	NE	NE
ESA treatment (High EpoR)	No	32	4	Referent		
	Yes	20	9	00291	3.41 (1.05-11.08)	0.0413

*Comparison made using the Wald Test. All p values are two-sided. NE=numbers not adequate for analysis.

SUPPLEMENTARY EXPERIMENTAL PROCEDURES

Description of all the materials used in the experiments described below.. All experiments were repeated at least twice.

Cell lines, maintenance and transfection reagents. All cell lines were maintained in 5% CO_2, 95% air at 37°C. Ovarian (HeyA8, SKOV3, A2780, RMG-2) and breast (MDA-MB231, MCF-7) cancer cells were obtained from the ATCC and human leukemic UT-7 cells are from DSMZ (cell line repository in Germany). The ovarian cell lines were maintained in DMEM with 15% heat-inactivated fetal bovine serum (FBS), while breast cell lines were maintained in DMEM with 5% FBS. Culture media was supplemented with 0.1% gentamicin sulfate (Gemini Bioproducts, Calabasas, CA). Cos-1 cells were maintained in 10% DMEM. UT-7 cells were maintained in 10% DMEM and GM-CSF (1ng/ml). All cell lines were routinely tested to confirm the absence of Mycoplasma (Gen-Probe detection kit; Thermo Fisher Scientific), and all *in vitro* experiments were conducted with 60-80% confluent cultures. In the *in vitro* experiments where the rhEpo dosage is not specified, the cell lines were treated with rhEpo 50 IU/ml.

***In vitro* siRNA and shRNA transfections.** All cell lines were transfected with Lipofectamine 2000 reagent (Invitrogen) using either siRNAs or shRNAs (Sigma-Aldrich) as specified in Table S11 according to the manufacturers protocol. Cells were stimulated with rhEpo (50 U/mL) after 48 hours of transfection.

Real time PCR analysis. Both cell line and tumor tissue total RNA was extracted using Qiagen RNeasy Kit (Qiagen, Valencia, CA). Using 500 ng of RNA, cDNA was synthesized by using a Verso cDNA kit (Thermo Scientific) as per the manufacturer's instructions. cDNA was subjected to amplification by real-time PCR using specific primer sequences as specified in Table S11. For real-time RT-PCR, we obtained quantitative values (each sample was normalized on the basis of its 18S content), as previously described (Thaker et al., 2006).

Protein analysis. For immunoblotting, lysates from cultured cells were prepared using modified RIPA buffer (50 mM Tris–HCl [pH 7.4], 150 mM NaCl, 1% Triton, 0.5% deoxycholate) plus 25 μg/mL leupeptin, 10 μg/mL aprotinin, 2 mM EDTA, and 1 mM sodium orthovanadate. To prepare lysates of snap-frozen tissue from mice, approximately 30-mm^3 cuts of tissue were disrupted with a tissue homogenizer and centrifuged at 13,000 rpm for 30 min within modified RIPA buffer. The protein concentrations were determined using a BCA Protein Assay Reagent kit (Pierce Biotechnology, Rockford, IL). Lysates were loaded and separated on 8% sodium dodecyl sulfate polyacrylamide gels. Proteins were transferred to a nitrocellulose membrane by semi-dry electrophoresis (Bio-Rad Laboratories, Hercules, CA) overnight, blocked with 5% milk for 1 hour and then incubated at 4°C with primary antibody overnight. After washing with TBST, the membranes were incubated with horseradish peroxidase (HRP)-conjugated horse anti-mouse IgG (1:2000, GE Healthcare, UK) for 2 hours. HRP was visualized by use of an enhanced chemi-luminescence detection kit (Pierce). To confirm equal sample loading, the blots were probed with an antibody

specific for beta-Actin (0.1 µg/mL; Sigma). Densitometry was calculated using Image-J software. For immunoprecipitation and co-immunoprecipitation, cells were lysed in non-denaturing NP40 cell lysis buffer. The extracts were incubated (2 h at 4 °C) with A/G-conjugated Ab, and for IP the beads were washed twice with RIPA buffer, once with 0.5 M LiCl in 0.1 M Tris (pH 8.0), and once with PBS. Reactions were boiled in sample buffer, and proteins were then subjected to 10% SDS-PAGE and immunoblotting. Please refer to Table S11 for specific antibodies.

Cell growth, proliferation, and cell cycle analysis. Cell growth and proliferation were assessed in triplicates. The time-point for rhEpo treatment (50 IU/mL) was 48 hours after siRNA transfection and incubation was for an additional 24 hours before analysis of cell proliferation. The cells were treated with EphrinB2 (2 ng/µL) for 48 hours to study the effect of EphrinB2 on proliferation. Cell proliferation was assessed with the Edu proliferation assay kit (Click-iT® Edu Alexa Fluor® 488 Flow Cytometry Assay Kit (Invitrogen), as described previously(Thaker et al., 2006). For cell cycle analysis, cells were lifted with Trypsin, washed with PBS and fixed in 70% cold ethanol and stored overnight at -20°C. Cells were then centrifuged (pelleted) at 1,200 rpm for 10 minutes at 4°C. After one wash with PBS cells suspended in propidium iodide (Roche) at 50 µg/mL and RNAse A (Qiagen) at 100 µg/mL and incubated in the dark at room temperature. Cells were then assessed for cell cycle phase by a Beckman Coulter XL 4-color flow cytometer. For testing EphB4 expression at different stages of cell cycle, cells were plated at density of 4×10^6 in 175 cm^2 plate 1 day before the experiment. Cells were

flow sorted according to cell cycle phases (G1, S and G2) using propidium iodide staining and DNA content analysis.

ELISA Assays. Protein levels were quantified by ELISA according to the manufacturer's protocol; please refer to Table S11 for specific ELISA assays. At time of assay, samples were thawed and centrifuged at 14,000 rpm at 4 ºC for 5 minutes and then stored on ice. The samples were assayed in triplicate or quadruplicate and data represents the mean concentration.

Invasion and Migration assays. Using modified Boyden chambers (Costar, Boston, MA) coated with either defined matrix (invasion) or 0.1% gelatin (migration), Untreated cells (7.5×10^4) cells for migration and 10^4 for invasion suspended in 100 µL serum-free media were added into the upper chamber. Complete media containing 10% FBS (500 µL) was added to the bottom chamber as a chemo-attractant. The chambers were incubated at 37ºC in 5% CO_2 for either 6 (migration) or 24 (invasion) hours. For siRNA knockdown studies, cells were treated with siRNA 48 hours prior to seeding cells in the Boyden chamber and cells were treated with rhEpo at the time of seeding. The cells were treated with EphrinB2 (2 ng/µL) to study the effect of EphrinB2 on invasion (24 hr) and migration (6 hr). After incubation, the cells in the upper chamber were removed with cotton swabs. Cells were fixed and stained and counted by light microscopy. Cells from 5 random fields were counted. Experiments were done in duplicates and performed three times.

Structure of Biological Macromolecules. Structural representations of EphB4:EphrinB2 complex (PDB: 1HLE) and EpoR:Epo complex (PDB:1CN4) were created with YASARA, YASARA Biosciences GmbH, Wagramer Strasse 25/3/45, 1220 Vienna, Austria.

Alignment between N-terminal domains of Ephb4 and Epo receptor. The sequence of the inhibitory peptide derived from EphB4 is highlighted in yellow, the homology region is boxed. Pairwise alignments were created with ClustalW (Larkin et al., 2007).

```
sp|P54760|EPHB4_HUMAN       ---MELRVLLCWASLAAALEETLLNTKLETADLKWVTFPQVDGQW--EEL 45
sp|P19235|EPOR_HUMAN        MDHLGASLWPQVGSLCLLLAGAAWAPPPNLPDPKFESKAALLAARGPEEL 50
                               :   :    .**.  *  :   .  : .* *: : . : .    ***

sp|P54760|EPHB4_HUMAN       SGLDEEQHSVRTYEVCDVQRAPGQAHWLRTGWVP----RRGAVHVYATLR 91
sp|P19235|EPOR_HUMAN        LCFTERLEDLVCFWEEAASAGVGPGNYSFSYQLEDEPWKLCRLHQAPTAR 100
                              : *. ..:  :    .. . * .::  :  :    :   :*  .* *

sp|P54760|EPHB4_HUMAN       FTMLECLSLPRAGRSCKETFTVFYYESDADTATALTPAWMENPYIKVDTV 141
sp|P19235|EPOR_HUMAN        GAVRFWCSLPTADTS---SFVPLELRVTAASG---APRYHRVIHINEVVL 144
                             ::    *** *. *   :*. :  .  * :.   :* : .  :*:  .:

sp|P54760|EPHB4_HUMAN       AAEHLTRKRPGAEATGKVNVKTLRLGPLSKAGFYLAFQD 180
sp|P19235|EPOR_HUMAN        LDAPVGLVARLADESGHVVLRWLPP-PETPMTSHIRY—180
                                :     *: :*:* :: *   * :    :: :
```

***In vivo* experiments.** For the dose-response effect of erythropoietin on tumors, respective groups were treated with 0, 50, or 200 IU of rhEpo by intraperitoneal administration three times weekly. For therapeutic experiments, treatment began 7 days after cell line injection. Treatment continued until mice in any group became moribund, at which point all were sacrificed, necropsied, and tumors were harvested. Tumor weights, number and location of tumor nodules were recorded. Tumor tissue was either

fixed in formalin for paraffin embedding, frozen in optimal cutting temperature (OCT) media to prepare frozen slides, or snap frozen for lysate preparation. Immediately before sacrificing the mice, blood samples were collected under anesthesia by cardiac puncture for standard complete blood count analysis evaluated by MD Anderson Department of Veterinary Medicine and Surgery lab services. For breast cancer models (MCF-7, MDA-MB231) and EphB4 negative ovarian cancer model (RMG2), three times weekly treatments of rhEpo (50 IU) were also started 7 days following injection of tumor cells and continued for the duration of the experiment.

Nanoparticle preparation and siRNA delivery. Tumor implantation, siRNA incorporation into DOPC-based nanoliposomes and delivery *in vivo* was carried out as previously described (Ahmed et al., 2010; Landen et al., 2007). DOPC and siRNA were mixed in the presence of excess tertiary butanol at a ratio of 1:10 (w/w) siRNA/DOPC. Tween 20 was added to the mixture in a ratio of 1:19 Tween 20: siRNA/DOPC. The mixture was vortexed, frozen in an acetone/dry ice bath and lyophilized. Before in vivo administration, this preparation was hydrated with PBS at room temperature at a concentration of 150 µg siRNA/kg/mouse. Chitosan nanoparticles (CH-NP) were prepared based on ionic gelation of anionic tripolyphosphate and siRNA. Briefly, predetermined tripolyphosphate (0.25% w/v) and siRNA (1 µg/µL) were added in chitosan solution, and the siRNA/CH-NP were spontaneously formed under constant stirring at room temperature. After incubation at 4°C for 40 minutes, siRNA/CH-NP was collected by centrifugation (Thermo Biofuge, Germany) at 13,000 rpm for 40 minutes at 4°C. The pellet was washed by sterile water three times to isolate siRNA/CH-NP, which

was stored at 4°C until used. For each of these experiments mice (10 mice per group) were randomly divided and treated with siRNA incorporated in neutral nanoliposomes (i.p. administration). For ovarian cancer models, twice weekly treatments started one week after cell injection and continued for approximately 4-6 weeks.

Construction of the Tissue Microarrays. Tissue microarray blocks were constructed by taking core samples from morphologically representative areas of paraffin embedded tumor tissues and assembling them on a recipient paraffin block with a precision instrument (Beecher Instruments, Silver Spring, MD) as described previously(Zhang et al., 2012) . The final tissue microarray consisted of 3 blocks with 179 available samples. All samples were spaced 0.5 mm apart. Five-micrometer sections were obtained from the microarray and stained with hematoxylin and eosin to confirm the presence of tumor and to assess tumor histology. Tumor samples were arranged randomly on the blocks. Sample tracking was based on coordinate position for each tissue spot in the tissue microarray block. The spots were transferred onto tissue microarray slides for staining. This sample tracking system was linked to a Microsoft Access database that contained demographic, clinicopathologic, and survival data on the patients who provided the samples, thereby allowing rapid links between histologic data and clinical features. The array was read according to the given tissue microarray map; each core was scored individually. Samples in which no tumor was found or no cores were available were excluded from the final data analysis.

Immunohistochemical analysis of EphB4, EpoR and IL6rb. Staining was performed in formalin-fixed, paraffin embedded tumor sections (4 µm thickness). After deparaffinization, rehydration and antigen retrieval or fixation, 3% H_2O_2 was used to block the endogenous peroxidase activity for 10 minutes. Protein blocking of non-specific epitopes was done using either 5% normal horse serum (Epo-R), 5% Bovine Serum Albumin (BSA) in 1x Tris buffered saline with 0.1% Tween 20 (TBST) (EphB4) or 4% fish gelatin in PBS (IL6Rb). Slides were incubated with primary antibody for Epo-R (1:25), EphB4 (1:500) (ab66336 for human tissue; AF446 for rat tissue) or IL6Rb (1:500) overnight at 4 ºC. After washing with PBS, the appropriate amount of horseradish peroxidase-conjugated secondary antibody was added and visualized with 3,3'-diaminobenzidine chromogen and counterstained with Gill's hematoxylin #3.

Transcription factor for analyzing DNA-binding activity of STAT3. The effect of rhEpo in stimulating STAT3-DNA binding was determined with TransCruz™ oligonucleotide agarose conjugated to the consensus binding site for Stat3 (Santa Cruz Inc., CA)(Yu et al., 1995). Nuclear extracts were made from A2780-shEpoR and A2780-shEphB4 cells that were pre-treated with rhEpo (10 U/mL). The bound STAT3 was separated by NuPAGE (Invitrogen, Carlsbad, CA) and immunoblotted with anti-STAT3 monoclonal antibody (Cell Signaling, MA). Densities of gel bands were determined by ImageJ software. The error-bar stands for the s.e.m. from three individual measurements.

***In silico* analysis.** We reasoned that any novel Epo receptor involved in mediating Epo's neuroprotective effect may also possess the two membrane proximal fibronectin 3 (FN3) domains (as found in EpoR). This fact is consistent with the domain architecture of many other hematopoietic cytokine binding proteins. Such conserved domain architecture is also compatible with both a heterodimeric complex containing EpoR and/or an independent homodimeric receptor. We thus extracted all proteins containing two membrane proximal FN3 domains from the human proteome (64 in all) and asked whether there was any evidence for their role in response to low oxygen conditions/ischemia. This regulatory aspect was analyzed because of the EpoR-independent tissue protective effects of Epo mutants. The latter analysis was performed using a text-mining approach that encompasses the use of comprehensive protein synonyms, and concepts such as hypoxia and ischemia. Of the 64 proteins containing the 2FN3-TM domain composition, only five showed evidence for mediating response to low oxygen conditions: *EPHB4, IL6RB, TIE1* and *TF* and *GHR*. Next, we asked which of these proteins had a reported role in Angiogenesis and/or erythropoiesis. These analyses were performed using a simple PUBMED query "Protein_name AND (Angiogenesis OR Erythropoiesis)". Only *EPHB4* and *IL6RB* possessed at least some evidence of involvement in both biological processes. Interestingly, *IL6RB* was considered a positive internal control in this process as it had already been reported that it may be involved in mediating Epo's tissue protective functions.

Interestingly, direct examination of the *EPHB4* locus revealed that it directly juxtaposes the Epo locus, albeit on the opposite strand. This close genomic association was conserved in all vertebrate genomes examined. Also interesting was the realization that

EPHB3 directly juxtaposes *THPO*, an association that is also conserved amongst species. Moreover, such genomic co-localization of functionally associated molecules is seen for other receptor:ligand partners (e.g. MST1 and its receptor MST1R: see http://www.ensembl.org/Homo_sapiens/contigview?gene=OTTHUMG00000136237;db=vega).

List of peptides used in competitive binding assays

Description	Localization	Sequence	Competitive Inhibition
TKL	23-41	TKLETADLKWVTFPQVDGQ	-
EEL	43-58	EELSGLDEEQHSVRTY	+
VQR	63-71	VQRAPGOAH	-
WVP	77-87	WVPRRGAVHVY	-
CLS	97-107	CLSLPRAGRSC	-
DAD	119-136	DADTATALTPAWMENPY	-
LRL	164-174	LRLGPLSKAGF	-
VPA	228-239	VPAPGPSPSLYC	-
EDG	241-252	EDGQWAEQPVTG	-
APG	256-267	APGFEAAEGNTK	-
FKP	267-287	FKPLSGEGSCQP	-
REC	362-373	RECRPGGSCAPC	-
DPG	380-389	DPGPRDLVEP	-
LNG	409-421	LNGVSSLATGPVP	-
EKG	473-483	EKGAEGPSSVR	-
RGL	496-505	RGLKRGASYLV	-
NCQ	Adam 15-EM		-
PPR	Epo 28-43		-

Detailed description of reagents used in this study

a. Antibodies

Antibody	Application	Vendor/Cat.No.
Epo	WB	R&D Systems (MAB2871)
EphB4	WB, IP, IHC	Invitrogen (37-1800) AbCam (ab66336) Thermoscientific (MA5-15506) R&D Biosystems (AF446)
EphB2	WB	AbCam (ab5418)
p-Tyr	WB	Invitrogen
EpoR	WB	Santa Cruz (sc-697)
Jak-2	WB	Cell Signaling (3230)
pJak-2	WB	Cell Signaling (3771)
STAT3	WB	Cell Signaling (4904)
pSTAT3	WB	Cell Signaling (9145)
STAT5	WB	Cell Signaling (9363)
pSTAT5	WB	Cell Signaling (4322)
Src	WB	Cell Signaling (2108)
EpoR-biotinylated	IHC	R&D Systems (BAF1390)
IL6Rb	IHC	AbCam (ab170257)

b. Assay Kits

Description	Species	Vendor/Ca.No.
Serum Epo ELISA	Human	R & D Systems/DEP00
Serum Epo ELISA	Mouse	R & D Systems/MEP00
pSTAT3 ELISA	Human	R & D Systems/KCB4607
pJak-2 ELISA	Human	Life Technologies/KHO5621
pSTAT5 ELISA	Human	R & D Systems/KCB4190

c. siRNA

Vendor	Sequence (5'-3')
Control sense	UUCUCCGAACGUGUCACGU [dT][dT]
Control antisense	ACGUGACACGUUCGGAGAA [dT][dT]
EpoR sense	GAUGAUCAGGGAUCCAAUA [dT][dT]
EpoR antisense	UAUUGGAUCCCUGAUCAUC [dT][dT]
EphB4 seq #1 sense	GAUCUGAAGUGGGUGACAU [dT][dT]
EphB4 seq #1antisense	AUGUCACCCACUUCAGAUC [dT][dT]
EphB4 seq #2 sense	CCCAUUUGAGCCUGUCAAU [dT][dT]
EphB4 seq #2antisense	AUUGACAGGCUCAAAUGGG [dT][dT]
EphB4 seq #3 sense	GAUCUGAAGUGGGUGACAU [dT][dT]
EphB4 seq #3antisense	AUGUCACCCACUUCAGAUC [dT][dT]
Src sense #1	GGCUGAGGAGUGGUAUUUU[dT][dT]
Src antisense #1	AAAAUACCACUCCUCAGCC[dT][dT]
Src sense #2	GCGAACCACCUGAACAAtt[dT] [dT]
Src antisense #2	UUGUUCAGGUGGUUCGCcc[dT] [dT]
STAT3 sense #1	GCCUCUCUGCAGAAUUCAA[dT][dT]
STAT3 antisense #1	UUGAAUUCUGCAGAGAGGC[dT][dT]
STAT3 sense #2	GGAUAACGUCAUUAGCAGA[dT] [dT]
STAT3 antisense #2	UCUGCUAAUGACGUUAUCC[dT] [dT]

d. shRNA

	Sequence
EpoR #1	CCGGCACCTAAAGTACCTGTACCTTCTCGAGAAGGTAC AGGTACTTTAGGTGTTTTTG
EpoR #2	CCGGGATGATCAGGGATCCAATATGCTCGAGCATATT GGATCCCTGATCATCTTTTTG
EphB 4 #1	CCGGCTGGAGTTACGGGATTGTGATCTCGAGATCACA ATCCCGTAACTCCAGTTTTT
Ephb 4 #2	CCGGCACCACCAAACTCAATCATTTCTCGAGAAATGAT TGAGTTTGGTGGTGTTTTTG

e. Primers

Oligo Name	Sequence 5'-3'
humEphB4 for	CGGCAGCCTCACTACTCAG
humEphB4 rev	TCCCATTTTGATGGCCCGAAG
humEpoR for	GATACCTATCTGGTGCTGGA
humEpoR rev	CTGTTCTCATAAGGGTTGGA
Mutated EphB4 for	CCTGCCAGCCATGCCCCGCGAACAGTCATT CTAACACCATTGGATCAG
Mutated EphB4 rev	CTGATCCAATGGTGTTAGAATGACTGTTCGC GGGGCATGGGCTGGCAGG
ß-Actin for	ATCTGGCACCACACCTTCTACAATGAGCTGC G
ß-Actin rev	CGTCATACTCCTGCTTGCTGATCCACATCTG C
STAT3 for	CTTCATTTCCCGTAAATCCCTAAAGCT
STAT3 rev	AGCTTTAGGGATTTACGGGAAATGA

f. cDNA

Name	Vendor	Catalog No.
EphB4	Origene	RG208559
EpoR	Origene	RG211341
Empty vector	Origene	PS100010

g. Chemicals

Name	Application	Vendor/Cat.No.
Soluble EphB4	Binding assay	R&D (10235-HCCH-200)
Soluble EphrinB2	Binding assay	Sino Biologicals (10881-HCCH-100)
Recombinant Epo	Binding assay	Genway
Procrit	*In vitro and in vivo*	Amgen
I^{125}-Epo	Binding assay	PerkinElmer
IL3	Binding assay	R&D (203-IL-050)
CXCL12	Binding assay	R&D (644-SD-025/CF)
PP2	*In vitro*	Sigma Aldrich
EPO/Fc	Binding assay	Cell sciences (CRE600C)
EPO/Fc	Binding assay	Cell sciences (CRE600B)
EPO-alpha/Fc	Binding assay	Cell sciences (CSI20107B)
EPO-beta/Fc	Binding assay	Cell sciences (CRE130A)
EPHB4/Fc	Binding assay	Biomiga (EB1004-200)
EFNB2 / Fc	Binding assay	Sino Biological Inc. (10881-H03H)
soluble EpoR	Binding assay	R&D (307-ER/CF)
EpoR/Fc	Binding assay	R&D (963-ER)

h. Agarose-beads conjugated STAT3 consensus oligos

Name	Vendor
5'— *GAT CCT TCT GGG AAT TCC TAG ATC* — 3' 3'— *CTA GGA AGA CCC TTA AGG ATC TAG* — 5'	Santa Cruz

SUPPLEMENTARY REFERENCES:

Ahmed, A. A., Lu, Z., Jennings, N. B., Etemadmoghadam, D., Capalbo, L., Jacamo, R. O., Barbosa-Morais, N., Le, X. F., Vivas-Mejia, P., Lopez-Berestein, G.*, et al.* (2010). SIK2 is a centrosome kinase required for bipolar mitotic spindle formation that provides a potential target for therapy in ovarian cancer. Cancer cell *18*, 109-121.

Landen, C. N., Jr., Lin, Y. G., Armaiz Pena, G. N., Das, P. D., Arevalo, J. M., Kamat, A. A., Han, L. Y., Jennings, N. B., Spannuth, W. A., Thaker, P. H.*, et al.* (2007). Neuroendocrine modulation of signal transducer and activator of transcription-3 in ovarian cancer. Cancer Res *67*, 10389-10396.

Larkin, M. A., Blackshields, G., Brown, N. P., Chenna, R., McGettigan, P. A., McWilliam, H., Valentin, F., Wallace, I. M., Wilm, A., Lopez, R.*, et al.* (2007). Clustal W and Clustal X version 2.0. Bioinformatics *23*, 2947-2948.

Thaker, P. H., Han, L. Y., Kamat, A. A., Arevalo, J. M., Takahashi, R., Lu, C., Jennings, N. B., Armaiz-Pena, G., Bankson, J. A., Ravoori, M.*, et al.* (2006). Chronic stress promotes tumor growth and angiogenesis in a mouse model of ovarian carcinoma. Nat Med *12*, 939-944.

Yu, C. L., Meyer, D. J., Campbell, G. S., Larner, A. C., Carter-Su, C., Schwartz, J., and Jove, R. (1995). Enhanced DNA-binding activity of a Stat3-related protein in cells transformed by the Src oncoprotein. Science *269*, 81-83.

Zhang, J., Guo, X., Chang, D. Y., Rosen, D. G., Mercado-Uribe, I., and Liu, J. (2012). CD133 expression associated with poor prognosis in ovarian cancer. Mod Pathol *25*, 456-464.